Motion Control of Swedish Wheeled Mobile Robots in the Presence of Actuator Saturation

Giovanni Indiveri[1], Jan Paulus[2], and Paul G. Plöger[2]

[1] DII Dipartimento Ingegneria Innovazione, University of Lecce, Lecce, Italy
giovanni.indiveri@unile.it
http://persone.dii.unile.it/indiveri/
[2] Univ. Apl. Science Bonn-Rhein-Sieg and Fraunhofer AIS
Sankt Augustin, Germany
http://www.inf.fh-bonn-rhein-sieg.de
http://www.ais.fraunhofer.de

Abstract. Swedish wheeled mobile robots have remarkable mobility properties allowing them to rotate and translate at the same time. Being holonomic systems, their kinematics model results in the possibility of designing separate and independent position and heading trajectory tracking control laws. Nevertheless, if these control laws should be implemented in the presence of unaccounted actuator saturation, the resulting saturated linear and angular velocity commands could interfere with each other thus dramatically affecting the overall expected performance. Based on Lyapunov's direct method, a position and heading trajectory tracking control law for Swedish wheeled robots is developed. It explicitly accounts for actuator saturation by using ideas from a prioritized task based control framework.

1 Introduction

In the last few years Swedish wheeled omnidirectional mobile robots have had a large attention among the mobile robotics research community. A Swedish wheel differs from a common wheel in the fact that rollers are mounted on its perimeter. If all the rollers are parallel to each other and misaligned with respect to the wheel hub axis, they will provide an extra degree of mobility with respect to a traditional perfectly rolling wheel. As reported in [1], the Swedish (or mecanum) wheel was invented in 1973 by Bengt Ilon, an engineer working for the Swedish company Mecanum AB. The interest in such kind of wheels is related to the possibility of developing omnidirectional robots in the sense of [2], i.e. robots that "have a full mobility in the plane which means that they can move at each instant in any direction without any reorientation" [2]. Notice that several references make a misleading use of the term omnidirectional, as they refer to vehicles equipped with fully steering traditional wheels. Such systems can eventually move in any direction, as the unicycle model, but only after reorienting their wheels appropriately and not at any given instant of time. The need to reorient the wheels or not prior to implementing any desired linear velocity is related to the presence or not of nonholonomic constraints. As

G. Lakemeyer et al. (Eds.): RoboCup 2006, LNAI 4434, pp. 35–46, 2007.

opposed to traditional wheel car-like or differentially driven mobile robots, the translational velocity vector of a Swedish wheeled vehicle can point in an arbitrary direction at any time without re-orienting the wheels. Otherwise stated, Swedish wheeled vehicles are not affected by nonholonomic constraints: as far as the structural properties of the kinematics model of a Swedish wheeled robot is concerned, angular and linear velocities are independent. As a consequence one can design separate and independent trajectory tracking guidance control laws for position and heading. Yet if these control laws are implemented in the presence of unaccounted actuator saturation, the resulting saturated linear and angular velocity commands could interfere with each other and thus affect the overall performance of the motion control schema. A novel trajectory tracking control law is presented in this paper that explicitly accounts for actuator saturation within a prioritized task approach. Heading and position tracking are treated as independent control objectives (tasks) having different priorities: by allocating control effort to the different tasks based upon their assigned priorities it is possible to guarantee the independence of the heading and position control actions in spite of actuator saturation. Overall convergence of tracking errors to zero is theoretically guaranteed using Lyapunov methods. In a RoboCup scenario priorities are an immediate consequence of the currently active behaviour roles taken by the robot. In the defend mode, by example, we want to block a ball as fast as possible thus maximum linear speed is called for, while during dribbling angular velocity takes the highest priority.

After deriving and discussing the vehicle's kinematics model in Section 2, a kinematics (guidance control) tracking control law accounting for actuator saturation is designed in Section 3 based on Lyapunov techniques. Experimental validation results are reported in Section 4. Final remarks and conclusions are discussed in Section 5.

2 Robot Kinematics Modeling

With reference to Fig. 1, a three wheel omnidrive mobile robot is considered. All wheel main axis, i.e. hub axis, are assumed to always lie parallel to a fixed ground plane $\mathcal{P}$ having unit vector $\mathbf{k} \perp \mathcal{P}$. An orthonormal body fixed frame $< B >= \{\mathbf{i}_B, \mathbf{j}_B, \mathbf{k}_B\}$ is chosen such that $\mathbf{i}_B \times \mathbf{j}_B = \mathbf{k}_B = \mathbf{k}$. Let $\mathbf{b}_h \; \forall \; h = \{1, 2, 3\}$ denote the position of the $h-$ths wheel hub in the body fixed frame and $\mathbf{n}_h$ the unit vector of each wheel hub axis, i.e. $\mathbf{n}_h := \mathbf{b}_h / \|\mathbf{b}_h\|$. At last for each wheel we define the unit vector $\mathbf{u}_h := \mathbf{n}_h \times \mathbf{k}$. Calling $\mathbf{v}_c$ the linear velocity of the robots center and $\omega \, \mathbf{k}$ its angular velocity vector, the velocity vector $\mathbf{v}_h$ of the center of each omnidirectional wheel hub will be given by:

$$\mathbf{v}_h = \mathbf{v}_c + \omega \, \mathbf{k} \times \mathbf{b}_h \quad \forall \;\; h = \{1, 2, 3\} \tag{1}$$

implying:

$$\mathbf{v}_c = \frac{1}{3} \left(\sum_{h=1}^{3} \mathbf{v}_h \; - \; \omega \, \mathbf{k} \times \sum_{h=1}^{3} \mathbf{b}_h \right) . \tag{2}$$

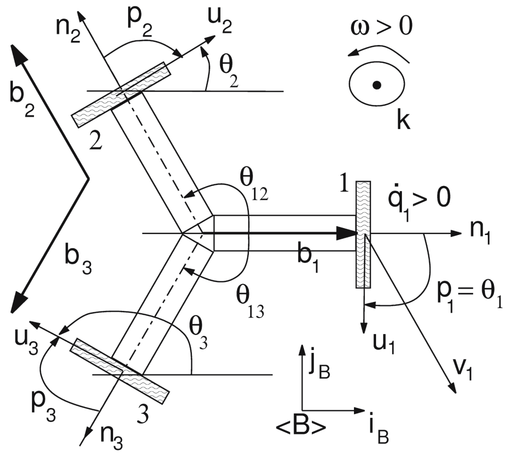

Fig. 1. Three wheel omnidrive robot: geometrical model

Based on this equation and on the non skidding hypothesis

$$\mathbf{v}_h^T \mathbf{u}_h = \rho\, \dot{q}_h \quad \forall \;\; h \tag{3}$$

where ρ is the wheel's radius (all wheels are assumed to have equal radius ρ) and $\dot{q}_h\, \mathbf{n}_h$ its angular velocity component along the hub axis (rolling angular velocity), the vehicle kinematics model can be expressed through the linear and angular velocity jacobian matrices as:

$$^{B}\mathbf{v}_c = J_{lv}\, \dot{\mathbf{q}} \quad : \quad J_{lv} \in R^{2\times 3} \tag{4}$$

$$\omega = J_{\omega}\, \dot{\mathbf{q}} \quad : \quad J_{\omega} \in R^{1\times 3}. \tag{5}$$

where the superscript B in $^{B}\mathbf{v}_c$ indicates that the components of vector $J_{lv}\, \dot{\mathbf{q}}$ are given in the body fixed frame $< B >$. If the three wheels should be mounted symmetrically at 120^o degrees from each other at a same distance $b = \|\mathbf{b}_h\| \;\; \forall \; h = \{1, 2, 3\}$ from the robot's center, and assuming the body fixed frame $< B >$ to have its x axis $\mathbf{i}_B$ aligned with $\mathbf{n}_1$ ($\mathbf{k}_B$ is normal to the plane $\mathcal{P}$ and $\mathbf{j}_B$ such that $\mathbf{k}_B = \mathbf{i}_B \times \mathbf{j}_B$) as depicted in figure (1) it can be shown after lengthy, but straightforward kinematics calculations, that:

$$J_{\omega} = -\frac{\rho}{3\,b}\,(1 \quad 1 \quad 1) \tag{6}$$

$$J_{lv} = \frac{\rho}{3}\begin{pmatrix} 0 & \sqrt{3} & -\sqrt{3} \\ -2 & 1 & 1 \end{pmatrix}. \tag{7}$$

Similar kinematics derivations for 3 and 4 Swedish wheeled robots are discussed, by example, in [3] -[9]. It is important to notice that both J_{ω} and J_{lv} given in equations (6) and (7) are full rank and that

$$J_{lv}\, J_{\omega}^T = \mathbf{0}. \tag{8}$$

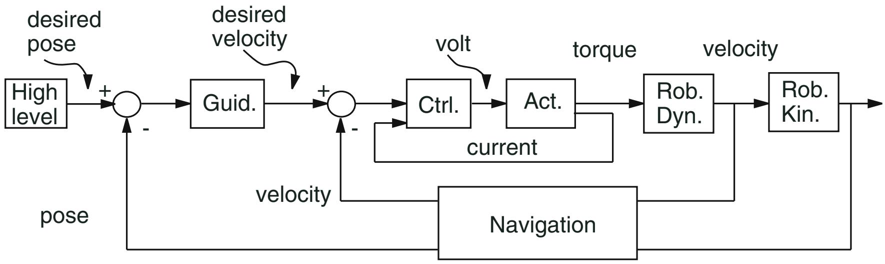

Fig. 2. Schematic view of an NGC architecture. Refer to text for details.

As shown in the sequel, this last equation allows to design separate kinematics control laws for linear and angular velocities. Interestingly the derivation of equations (6) and (7), here not reported for the sake of shortness, shows that property (8) is a consequence of having assumed the wheels to be symmetrically located, namely that $\sum_i \mathbf{b}_i = \mathbf{0}$.

3 Trajectory Tracking Control Law Design

Following a standard and most common approach for autonomous robots, the overall control architecture is organized on three level: navigation, guidance and control (NGC). Navigation takes care of the vehicles motion state estimation based upon available proprioceptive and exteroceptive information. Guidance is a closed loop control system, fed by the navigation subsystem, designed on the kinematics model of the system that generates desired angular and linear velocity reference signals. Within the described NGC framework, a trajectory tracking guidance law is derived: given an inertial (global) frame $< G >= (\mathbf{i}, \mathbf{j}, \mathbf{k})$ with $\mathbf{k} := (\mathbf{i} \times \mathbf{j}) \perp \mathcal{P}$ being $\mathcal{P}$ the floor plane, a reference (planar) trajectory is a differentiable curve in $\mathcal{P}$

$$\mathbf{r}_d(t) = \mathbf{i}\ \left(\mathbf{r}_d^T(t)\mathbf{i}\right) + \mathbf{j}\ \left(\mathbf{r}_d^T(t)\mathbf{j}\right) \tag{9}$$

with curvilinear abscissa

$$s(t) := \int_{t_0}^{t} \left\| \frac{d\,\mathbf{r}_d(\tau)}{d\tau} \right\| d\tau \tag{10}$$

and unit tangent vector

$$\mathbf{t}_d = \frac{d\,\mathbf{r}_d}{ds}. \tag{11}$$

The kinematics trajectory tracking problem consists in finding a control law for the systems input $\dot{\mathbf{q}}$ such that the position and heading tracking errors

$$\mathbf{e}_r(t) := \mathbf{r}_d(t) - \mathbf{r}_c(t) \tag{12}$$

$$e_\varphi(t) := \varphi_d(t) - \varphi(t) \tag{13}$$

converge to zero, namely such that:

$$\lim_{t\to\infty} \mathbf{e}_r(t) = \lim_{t\to\infty} (\mathbf{r}_d(t) - \mathbf{r}_c(t)) = 0 \tag{14}$$

$$\lim_{t\to\infty} e_\varphi(t) = \lim_{t\to\infty} (\varphi_d(t) - \varphi(t)) = 0 \tag{15}$$

being $\mathbf{r}_c(t)$ the position in $< G >$ of a reference point (e.g. the geometrical center or the center of mass) of the robot, $\varphi(t)$ its heading, $\varphi_d(t)$ the desired reference heading, $\mathbf{e}_r(t) = (\mathbf{r}_d(t) - \mathbf{r}_c(t))$ the position tracking error and $e_\varphi(t) = (\varphi_d(t) - \varphi(t))$ the heading error. Notice that for nonholonomic vehicles having a unicycle or car-like kinematics model, the reference heading $\varphi_d(t)$ is *not* arbitrary, but needs to coincide with the heading of the trajectories unit tangent vector $\mathbf{t}_d$. To the contrary given any position reference trajectory $\mathbf{r}_d(t)$, a Swedish wheeled vehicle will be free to track any arbitrary heading $\varphi_d(t)$ that does not need to coincide with the heading of $\mathbf{t}_d$.

3.1 Trajectory Tracking Controller Design

In accordance with the notation previously introduced, consider equations (4-5) being $\mathbf{v}_c = \dot{\mathbf{r}}_c(t)$ and $\omega = \dot{\varphi}(t)$ the time derivatives of the robots position $\mathbf{r}_c(t)$ and heading $\varphi(t)$. To solve the above stated trajectory tracking problem, consider the Lyapunov candidate function

$$V = \frac{1}{2}\mathbf{e}_r^T\, K_r\, \mathbf{e}_r + \frac{1}{2} e_\varphi^T\, K_\varphi\, e_\varphi \tag{16}$$

being $K_r \in R^{2\times 2}$ a symmetric positive definite ($K_r > 0$) matrix and K_φ a positive constant. The time derivative of V results in

$$\dot{V} = \mathbf{e}_r^T\, K_r\, (\dot{\mathbf{r}}_d(t) - J_{lv}\dot{\mathbf{q}}) + e_\varphi^T\, K_\varphi\, (\dot{\varphi}_d(t) - J_\omega \dot{\mathbf{q}})\,. \tag{17}$$

Denoting with $J_{lv}^\dagger$ and $J_\omega^\dagger$ the right pseudo-inverse matrices of full rank J_{lv} and J_ω respectively (J_{lv} and J_ω are full rank by hypothesis),

$$J_{lv}^\dagger = J_{lv}^T \left(J_{lv}\, J_{lv}^T\right)^{-1} \quad \text{and} \quad J_\omega^\dagger = J_\omega^T \left(J_\omega\, J_\omega^T\right)^{-1} \tag{18}$$

a possible value for $\dot{\mathbf{q}}$ making $\dot{V}$ in equation (17) negative definite is:

$$\dot{\mathbf{q}}_d(t) = \dot{\mathbf{q}}_{lvd}(t) \;+\; \dot{\mathbf{q}}_{\varphi d}(t) \tag{19}$$

$$\dot{\mathbf{q}}_{lvd}(t) = J_{lv}^\dagger\, (\, \dot{\mathbf{r}}_d(t) + K_r\, \mathbf{e}_r(t)\,) \tag{20}$$

$$\dot{\mathbf{q}}_{\varphi d}(t) = J_\omega^\dagger\, (\, \dot{\varphi}_d(t) + K_\varphi\, e_\varphi(t)\,) \tag{21}$$

implying in closed loop

$$\dot{V} = -\mathbf{e}_r^T\, K_r\, K_r\, \mathbf{e}_r - (K_\varphi\, e_\varphi)^2 < 0. \tag{22}$$

As for standard tracking controllers, the solution in equation (19) is a combination of feedforward terms proportional to the reference linear and angular velocities and a feedback term. The proposed solution guarantees global exponential stability of equilibrium $\mathbf{e}_r = \mathbf{0}, e_\varphi = 0$ of the error dynamics, thus (robustly) solving the trajectory tracking problem. Control law (19) is the sum of two contributions: the first (20) relative to position tracking and the second (21) to heading tracking. In the light of property (8), it should be noticed that the two contributions do not interfere with each other, namely the contribution of $\dot{\mathbf{q}}_{lvd}$ to the robots angular velocity and the contribution of $\dot{\mathbf{q}}_{\varphi d}$ to the robots linear velocity are both null, i.e.

$$J_\omega \dot{\mathbf{q}}_{lvd} = J_\omega \left(J_{lv}^T \left(J_{lv} J_{lv}^T \right)^{-1} \right) \left(\dot{\mathbf{r}}_d(t) + K_r \, \mathbf{e}_r(t) \right) = 0 \tag{23}$$

$$J_{lv} \dot{\mathbf{q}}_{\varphi d}(t) = J_{lv} \left(J_\omega^T \left(J_\omega J_\omega^T \right)^{-1} \right) \left(\dot{\varphi}_d(t) + K_\varphi \, e_\varphi(t) \right) = \mathbf{0} \tag{24}$$

due to the fact that they are proportional to $J_\omega J_{lv}^T$ and $J_{lv} J_\omega^T$ respectively. As discussed above, when designing vehicle kinematics guidance laws it must be assumed that the lower level (actuator) dynamics should be much faster than the kinematics. This requirement is reflected on design choices such as actuator power and desired reference trajectories: the former needs to be sufficiently large for the given inertial properties of the vehicle so that maximum vehicle accelerations can be much larger than the maximum reference accelerations $\ddot{\varphi}_d(t)$ and $\ddot{\mathbf{r}}_d(t)$. As far as the ratio of maximum vehicle acceleration over maximum reference acceleration is sufficiently large the dynamic behaviour of the kinematics guidance law will be fine. Thus, as for any other kinematics designed guidance solution, the proposed control law should be implemented on Swedish wheeled vehicles with sufficiently powerful actuators with respect to the maximum reference accelerations $\ddot{\varphi}_d(t)$ and $\ddot{\mathbf{r}}_d(t)$. As for actuator saturation, the situation is slightly more complex. Given the proportional nature of the control law (19), the tracking error (either in position or heading) or the desired reference velocities can always happen to be large enough for the actuators to saturate, namely calling $\dot{q}_{\max} > 0$ the maximum absolute angular velocity that the vehicles actuators are able to generate, whatever the gains K_r and K_φ should be, depending on $\dot{\varphi}_d(t)$, $\dot{\mathbf{r}}_d(t)$, $\mathbf{e}_r(t)$ or $e_\varphi(t)$ the saturation condition[1]

$$\|\dot{\mathbf{q}}_d\|_\infty \ \leq \ \dot{q}_{\max} \tag{25}$$

may always be violated. Notice that while the feedforward signals $\dot{\varphi}_d(t)$ and $\dot{\mathbf{r}}_d(t)$ can eventually always be bounded, the tracking error's initial conditions are not design parameters. Hence a commanded $\dot{\mathbf{q}}_d$ with exceeding infinity-norm due to odd initial conditions cannot be *a priori* excluded.

3.2 Actuator Saturation

The presence of actuator saturation has a severe impact on performance: in particular given the additive structure of equation (19), saturation can affect the decoupling between commanded angular and linear velocities. In order to

[1] Given $\mathbf{q} \in R^{N\times 1}$, $\|\mathbf{q}\|_\infty = \max\{|q_1|, |q_2|, \ldots, |q_N|\}$ is its infinity norm.

cope with actuator saturation and to guarantee a prioritized execution of the position and heading tracking tasks, the following modification of the proposed control law is suggested: the sum in equation (19) should be weighted with error and reference dependent weights such that (*i*) the resulting $\dot{\mathbf{q}}_d$ command has norm within the actuator limits, (*ii*) the tasks (position and heading in the present case) are executed with a priority based time order (higher priority tasks earlier) and (*iii*) the tracking error converges to zero.

To reach these goals, consider the saturation function

$$\sigma : R \times [0, \infty) \longrightarrow R \quad \text{such that} \quad \sigma(x, c) = \begin{cases} 0 & \text{if} \quad x = 0 \\ 1 & \text{if} \quad 0 < |x| < c \\ c/|x| & \text{otherwise.} \end{cases} \tag{26}$$

In the sequel the non negative second argument c of $\sigma(x, c)$ will be called the capacity of x. Notice that by definition $\sigma(x, c)$ is simply a nonnegative scalar scaling factor such that $x\,\sigma(x, c)$ is "clipped" to $c\,\text{sign}(x)$ whenever $|x|$ should exceed the capacity c and is equal to x otherwise, i.e. $x\,\sigma(x, c)$ is simply the saturated version of x in the range $[-c, c]$. Also notice that by its very definition

$$\sigma(x, 0) = 0 \ \ \forall \ \ x, \tag{27}$$

namely if x should be assigned zero capacity, then $x\,\sigma(x, 0) = 0$ for any value of x. Assume that

$$\dot{\mathbf{q}}_d = \sum_{l=1}^{n} \dot{\mathbf{q}}_l \tag{28}$$

is the actuator input being $\dot{\mathbf{q}}_1, \dot{\mathbf{q}}_2, \ldots, \dot{\mathbf{q}}_n$ n independent task inputs ordered by decreasing priority with increasing index ($\dot{\mathbf{q}}_1$ has highest priority). Each term on the right hand side of equation (28) and $\dot{\mathbf{q}}_d$ itself should be bounded by $\dot{q}_{\max}$. Considering that each task should be executed in a prioritized fashion, the sum in (28) may be replaced by a weighted sum as follows:

$$\dot{\mathbf{q}}_d = \dot{\mathbf{q}}_1\,\sigma\left(\|\dot{\mathbf{q}}_1\|_\infty, c_1\right) \ + \ \dot{\mathbf{q}}_2\,\sigma\left(\|\dot{\mathbf{q}}_2\|_\infty, c_2\right) \ + \ \ldots \ + \ \dot{\mathbf{q}}_n\,\sigma\left(\|\dot{\mathbf{q}}_n\|_\infty, c_n\right) \tag{29}$$

where each task capacity is recursively and dynamically computed as:

$$\begin{aligned} c_1(t) &\le \dot{q}_{\max} \quad (\text{constant, i.e. } \dot{c}_1(t) = 0) \\ c_2(t) &= c_1 - \|\dot{\mathbf{q}}_1\|_\infty\,\sigma\left(\|\dot{\mathbf{q}}_1\|_\infty, c_1\right) \\ c_3(t) &= c_2(t) - \|\dot{\mathbf{q}}_2\|_\infty\,\sigma\left(\|\dot{\mathbf{q}}_2\|_\infty, c_2(t)\right) \\ \vdots &= \vdots \\ c_n(t) &= c_{n-1}(t) - \|\dot{\mathbf{q}}_{n-1}\|_\infty\,\sigma\left(\|\dot{\mathbf{q}}_{n-1}\|_\infty, c_{n-1}(t)\right). \end{aligned} \tag{30}$$

$c_1, \ldots, c_n$ can be chosen according to the state of the environment, i.e. in RoboCup they can depend on global external game states. Notice that by construction all the above task capacities are non negative, i.e.

$$c_j \ge 0 \ \ \forall \ \ j \in [1, n],$$

and that

$$c_j \le c_{j-1} \quad \forall \quad j \in [2, n]$$
$$c_i = 0 \implies c_j = 0 \quad \forall \quad j > i$$

namely if a given task is assigned zero capacity, all the lower priority tasks will also automatically have zero capacity and all their weights in the sum (29) will be zero. The capacity of task i can be viewed as the residual capacity after the higher priority task $i-1$ has been commanded; thus, by example, c_2 will be zero (and also $c_j : j > 2$) if the task 1 input $\dot{\mathbf{q}}_1$ is saturating all its capacity c_1. In words, each task will be commanded with a non null weight only if the higher priority task have not saturated. The fact that c_1 needs not to exceed $\dot{q}_{\max}$ is due to the fact that task 1 alone should not saturate the actuator capacity $\dot{q}_{\max}$; moreover given that $c_{j+1} \le c_j \ \forall \ j \in [1, n-1]$ the condition $c_1 \le \dot{q}_{\max}$ guarantees that *each* term in the sum (29) will have infinity norm smaller or equal to the threshold $\dot{q}_{\max}$. Indeed the proposed dynamic update rule for the task's capacities also guarantees that the total control signal (29) has infinity norm smaller or equal than $\dot{q}_{\max}$. In order to implement the above described schema in the present trajectory tracking case, assume that the reference feedforward linear and angular velocities are sufficiently small, namely that

$$\left\| J_{lv}^{\dagger} \, \dot{\mathbf{r}}_d(t) \right\|_{\infty} < \frac{1}{2} \ \dot{q}_{\max} \quad \forall \, t \tag{31}$$

$$\left\| J_{\omega}^{\dagger} \, \dot{\varphi}_d(t) \right\|_{\infty} < \frac{1}{2} \ \dot{q}_{\max} \quad \forall \, t. \tag{32}$$

These conditions are necessary to guarantee that the tracking task is asymptotically feasible, namely that when the position and heading tracking errors are null the control effort of the control law (19) is compatible with the actuator saturation limit, i.e.

$$\mathbf{e}_r = \mathbf{0}, e_{\varphi} = 0 \quad \implies$$
$$\|\dot{\mathbf{q}}_d(t)\|_{\infty} = \left\| J_{lv}^{\dagger} \, \dot{\mathbf{r}}_d(t) + J_{\omega}^{\dagger} \, \dot{\varphi}_d(t) \right\|_{\infty} \le \left\| J_{lv}^{\dagger} \, \dot{\mathbf{r}}_d(t) \right\|_{\infty} + \left\| J_{\omega}^{\dagger} \, \dot{\varphi}_d(t) \right\|_{\infty} < \dot{q}_{\max}.$$

As a first example, assume that position tracking is assigned highest priority with respect to heading tracking. Then define:

$$\dot{\mathbf{q}}_1 := J_{lv}^{\dagger} \, \dot{\mathbf{r}}_d(t) \tag{33}$$
$$\dot{\mathbf{q}}_2 := J_{lv}^{\dagger} \, K_r \, \mathbf{e}_r(t) \tag{34}$$
$$\dot{\mathbf{q}}_3 := J_{\omega}^{\dagger} \, \dot{\varphi}_d(t) \tag{35}$$
$$\dot{\mathbf{q}}_4 := J_{\omega}^{\dagger} \, K_{\varphi} \, e_{\varphi}(t). \tag{36}$$

With these definitions consider the control law (29-30) with

$$c_1(t) = \dot{q}_{\max} > 0 \ \forall \ t$$

that together with the feasibility condition (31) implies

$$0 < \frac{1}{2} \, \dot{q}_{\max} \le c_2 \le \dot{q}_{\max},$$

i.e. the tasks 1 and 2 have always non null capacity. Moreover as by hypothesis $\|\dot{\mathbf{q}}_1\|_\infty < 0.5\,\dot{q}_{\max}$ (equation (31)) and $c_1 = \dot{q}_{\max}$, it follows that

$$\dot{\mathbf{q}}_1\,\sigma(\|\dot{\mathbf{q}}_1\|_\infty, c_1) = \dot{\mathbf{q}}_1 \quad \forall \quad t.$$

Consequently

$$\begin{aligned}
V_1 &= \frac{1}{2}\mathbf{e}_r^T\,K_r\,\mathbf{e}_r \quad \Longrightarrow \qquad (37)\\
\dot{V}_1 &= \mathbf{e}_r^T\,K_r\,\left(\dot{\mathbf{r}}_d(t) - J_{lv}\left[J_{lv}^\dagger\,\dot{\mathbf{r}}_d(t) + J_{lv}^\dagger\,K_r\,\mathbf{e}_r(t)\,\sigma\left(\left\|J_{lv}^\dagger\,K_r\,\mathbf{e}_r(t)\right\|_\infty, c_2\right)\right]\right) = \\
&= -\mathbf{e}_r^T\,K_r\,K_r\,\mathbf{e}_r(t)\,\sigma\left(\left\|J_{lv}^\dagger\,K_r\,\mathbf{e}_r(t)\right\|_\infty, c_2\right) < 0
\end{aligned}$$

i.e. $\dot{V}_1$ is negative definite that proves asymptotic global Lyapunov stability of $\mathbf{e}_r = \mathbf{0}$. Notice that $\dot{\mathbf{q}}_3$ and $\dot{\mathbf{q}}_4$ do not contribute to $\dot{V}_1$ as they belong to the null space of J_{lv} (equation 8). As far as the secondary (heading) task is concerned, convergence can also be proven through a Lyapunov argument. The global asymptotic stability of $\mathbf{e}_r = \mathbf{0}$ guarantees that

$$\lim_{t\to\infty}\dot{\mathbf{q}}_2(t) = \mathbf{0} \quad \Longrightarrow \quad \lim_{t\to\infty} c_3 = c_2 \;\geq\; \frac{1}{2}\dot{q}_{\max}.$$

Given the feasibility condition (32), this means that

$$\exists\; t^* \;\;:\;\; \dot{\mathbf{q}}_3\,\sigma(\|\dot{\mathbf{q}}_3\|_\infty, c_3) = \dot{\mathbf{q}}_3 \;\text{ and }\; c_4 > 0 \;\;\forall\;\; t \geq t^*.$$

It follows that

$$\begin{aligned}
V_2 &= \frac{1}{2}e_\varphi^T\,K_\varphi\,e_\varphi \quad \Longrightarrow \qquad (38)\\
\dot{V}_2(t)\Big|_{t\geq t^*} &= e_\varphi^T\,K_\varphi\,\left(\dot{\varphi}_d(t) - J_\omega\dot{\mathbf{q}}_d\right) = \\
&= e_\varphi^T\,K_\varphi\,\left[\dot{\varphi}_d(t) - J_\omega(J_\omega^\dagger\,\dot{\varphi}_d(t) + J_\omega^\dagger\,K_\varphi\,e_\varphi(t)\,\sigma\left(\left\|J_\omega^\dagger\,K_\varphi\,e_\varphi(t)\right\|_\infty, c_4\right))\right] = \\
&= -e_\varphi^T\,K_\varphi^2\,e_\varphi(t)\,\sigma\left(\left\|J_\omega^\dagger\,K_\varphi\,e_\varphi(t)\right\|_\infty, c_4\right) < 0
\end{aligned}$$

namely there exists a finite time t^* after which the time derivative of V_2 is always negative, thus proving convergence to zero of the heading error $e_\varphi(t)$. Prior to t^* the heading error $e_\varphi(t)$ is not guaranteed to be decreasing. Notice that $\dot{\mathbf{q}}_1$ and $\dot{\mathbf{q}}_2$ do not contribute to $\dot{V}_2$ as they belong to the null space of J_ω (equation 8).

As a second example, heading can be selected to be the highest priority task, it is then sufficient to select $\dot{\mathbf{q}}_1, \ldots, \dot{\mathbf{q}}_4$ as

$$\dot{\mathbf{q}}_1 := J_\omega^\dagger\,\dot{\varphi}_d(t) \qquad (39)$$

$$\dot{\mathbf{q}}_2 := J_\omega^\dagger\,K_\varphi\,e_\varphi(t) \qquad (40)$$

$$\dot{\mathbf{q}}_3 := J_{lv}^\dagger\,\dot{\mathbf{r}}_d(t) \qquad (41)$$

$$\dot{\mathbf{q}}_4 := J_{lv}^\dagger\,K_r\,\mathbf{e}_r(t) \qquad (42)$$

in equations (29-30); Lyapunov stability of the heading error and asymptotic convergence of the position error could be proven accordingly.

4 Experimental Results

The proposed control law has been experimentally tested on the Volksbot platform (*www.volksbot.de*) [10] developed at the Fraunhofer AiS - Autonomous intelligent Systems Institute of Sankt Augustin, Germany. The robot is about 8Kg in weight and is actuated by three 90 Watts, 24 volt DC motors with a 1 : 8 gear ratio. Low level wheel speed control is achieved through a 3 channel PID motor driver (the AiS TMC200 board) interfaced to an onboard laptop via a regular serial RS232 line. The presented kinematics trajectory tracking control law, i.e. the guidance loop in figure (2), is implemented on the onboard laptop. Motor power is supplied through NiMH batteries with $3,5$ Ah capacity. The three omnidirectional wheels have a 5cm radius, are made of lightweight plastic and are mounted at 120^o from each other. The robot is equipped with an omnivision system made by a 30Hz, 640×480 pixels YUV color FireWire camera pointing towards a 70mm diameter hyperbolic mirror. Such systems are used for map-based Monte Carlo self-localization [11] [13]. Details can be found in [12].

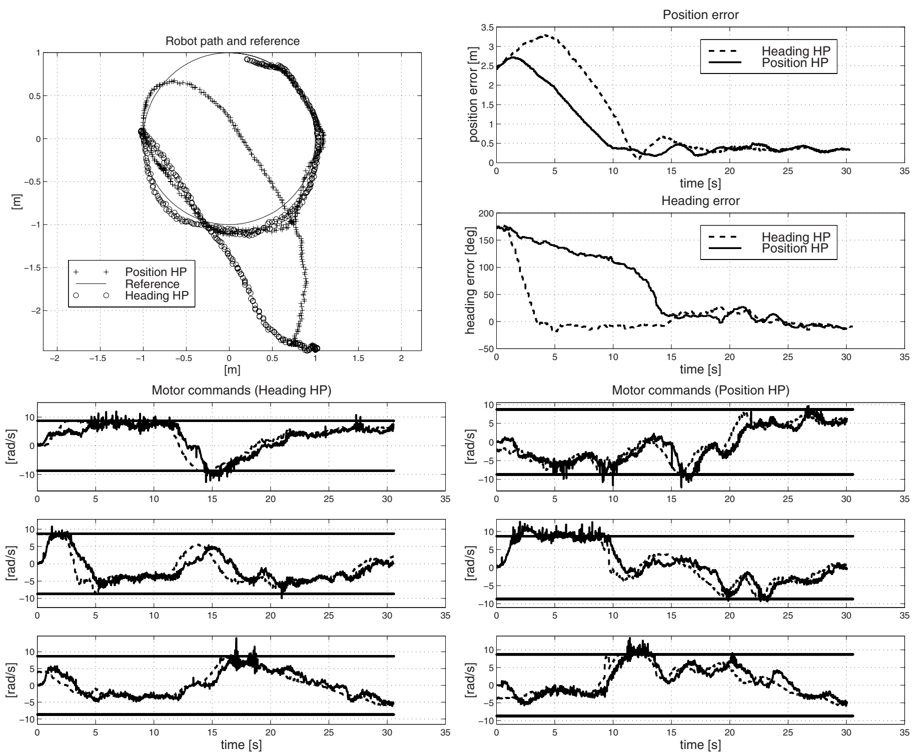

Fig. 3. Experimental results. HP stands for High Priority. Refer to text for details.

In order to evaluate the performance of the proposed control solution the position and heading of the robot must be measured reliably and compared with the desired reference values. To this extent an experimental setup has been designed where the position of the robot was measured by a fixed laser range finder pointing on the robot and its heading was measured by the robot itself using its omnivision system. All collected data was suitably synchronized with the desired references. Extensive experimental trials with several different references have shown the effectiveness of the proposed solution: the case of a circular reference trajectory with constant (with respect to a fixed frame) heading is reported in figure (3). The position and heading error plots with respect to time clearly confirm the effectiveness of the priority assignment policy. The growth of the position errors in the first few seconds of the experiment (top right plot) are due to the robots dynamics that was neglected in the control law design. As expected, as long as the actuators guarantee large enough accelerations with respect to the reference accelerations, the kinematics designed control law exhibits good dynamic performance, i.e. there is only a small lag with respect to the ideal purely kinematics case.

In the motor command plots, the commanded ($\dot{q}_d$, dashed lines) and encoder measured wheel speeds (solid lines) are reported with respect to time. Notice that for the sake of performance measurement accuracy, the saturation threshold was artificially set to the value of ±8.7rad/s (thick solid lines) via software in order to achieve saturation at acceptable linear speeds.

5 Conclusions

A trajectory tracking control law for Swedish wheeled robots has been derived that takes explicitly into account motor saturations. Motor saturation is always present and may have a sever impact on motion control performances of mobile robots. This is particularly relevant for omnidirectional mobile robots equipped with Swedish wheels: these offer a lower grip with the floor with respect to traditional wheels resulting in a higher probability of exhibiting skidding and/or sliding when high velocity commands are issued. As a consequence the possibility of commanding motor speeds always compatible with the saturation limits is extremely important for omnidirectional mobile robots. Moreover the introduction of a task based prioritization of heading and position tracking may have a relevant impact on the behaviour control level. The selection of heading or position tracking tasks as higher priority ones will generally depend on the (dynamic) role assignment: by using the described lower level control solution the highest priority tasks errors are guaranteed to converge faster to zero without ever commanding motor speeds exceeding the maximum HW allowed values. Future work directions should include studies on how the behaviour system should take advantage of a guaranteed prioritized convergence of the tracking errors.

References

1. Diegel, O., Badve, A., Bright, G., Potgieter, J., Tlale, S.: Improved Mecanum Wheel Design for Omni-directional Robots. In: Proc. 2002 Australian Conference on Robotics and Automation, Auckland, pp. 27–29 (November 2002)
2. Campion, G., Bastin, G., D'Andréa-Novel, B.: Structural Properties and Classification of Kinematic and Dynamic Models of Wheeled Mobile Robots. IEEE Transactions on Robotics and Automation 12(1), 47–62 (1996)
3. Agulló, J., Cardona, S., Vivancos, J.: Kinematics of Vehicles with Directional Sliding Wheels. Mech. Mach. Theory 22(4), 295–301 (1987)
4. Muir, P.F., Neuman, C.P.: Kinematic Modeling For Feedback Control Of An Omnidirectional Wheeled Mobile Robot. In: Cox, J., Wilfong, G.T. (eds.) Autonomous robot vehicles, pp. 25–31. Springer, New York (1990)
5. Pin, F.G., Killough, S.M.: A New Family of Omnidirectional and Holonomic Wheeled Platforms for Mobile Robots. IEEE Transactions on Robotics and Automation 10(4), 480–489 (1994)
6. Asama, H., Sato, M., Bogoni, L., Kaetsu, H., Matsumoto, A., Endo, I.: Development of an Omni-Directional Mobile Robot with 3 DOF Decoupling Drive Mechanism. In: Proc. of the 1995 IEEE International Conference on Robotics and Automation (ICRA 95), Nagoya, Aichi, Japan, pp. 1925–1930 (1995)
7. Loh, W.K., Low, K.H., Leow, Y.P.: Mechatronics Design and Kinematic Modelling of a Singularityless Omni-Directional Wheeled Mobile Robot: In: Proc. of the, IEEE International Conference on Robotics and Automation (ICRA 03), Tapei, Taiwan, September 14 - 19, 2003, pp. 3237–3242 (2003)
8. Kim, W.K., Yi, B.-J., Lim, D.J.: Kinematic Modeling of Mobile Robots by Transfer Method of Augmented Generalized Coordinates. Journal of Robotic Systems 21(6), 275–300 (2004)
9. Song, J.-B., Byun, K.-S.: Design and Control of a Four-Wheeled Omnidirectional Mobile Robot with Steerable Omnidirectional Wheels. Journal of Robotic Systems 21(4), 193–208 (2004)
10. Wisspeintner, T., Nowak, W., Bredenfeld, A.: Volksbot: A flexible component based mobile Robot system. In: ROBOCUP Symposium 2005, Springer LNAI, http://www.ais.fraunhofer.de/BE/2005/Wisspeintner_2005_RoboCup_VolksBot.pdf (to appear)
11. Menegatti, E., Pretto, A., Pagello, E.: A new omnidirectional vision sensor for monte-carlo localization. In: Int. RoboCup Symposium CD-ROM, Lisbon, Portugal (2004)
12. Olufs, S.: Vision-Based Probabilistic State Estimation using Omnidirectional Cameras. Master Thesis FH-BRS, St. Augustin (2005)
13. Schulz, D., Burgard, W., Fox, D., Cremers, A.: People tracking with a mobile robot using sample-based joint probabilistic data association filters. International Journal of Robotics Research (IJRR). Springer (2003)